SABA Publishing

Journal of Mathematical Analysis and Modeling
jmam.sabapub.com
ISSN 2709-5924

J Math Anal & Model
(2026)7(2) : 82-95
doi:10.48185/jmam.v7i2.2002

Stability Analysis and Approximation of Time Fractional Hyperbolic Integro Partial Differential Equations

FATIH OZBAG[a,*]

[a] Mathematics Department, Harran University, Sanliurfa, Turkey

• *Received: 21 February 2026* • *Accepted: 14 June 2026* • *Published Online: 25 October 2026*

Abstract

This paper presents first-order and second-order finite difference schemes for solving a class of fractional hyperbolic integro-partial differential equations involving a Caputo fractional derivative. The fractional derivative and integral terms are discretized using suitable numerical approximations, leading to a fully discrete system. Stability properties are investigated through a Fourier (von Neumann) analysis, and numerical experiments are performed to assess the accuracy and convergence of the proposed methods. Maximum norm errors and experimental orders of convergence are reported, confirming first-order convergence in both space and time. The numerical results further demonstrate that the second-order scheme provides significantly improved accuracy and agrees closely with the exact solution.

Keywords: Integro partial differential equation, Von Neumann stability, Caputo time fractional derivative, Approximate solution, Finite difference scheme
2010 MSC: 65M06, 65M12, 35R09, 35R11.

1. Introduction

Partial and ordinary differential equations are commonly used to express mathematical models in various fields, including physics, chemistry, engineering, biology, and economics [1, 2, 3]. Analyzing and solving these equations, both analytically and numerically, is crucial for understanding the phenomena being studied. There are three types of partial differential equations, and this study specifically focuses on the hyperbolic type.

Over the past few decades, there has been a significant interest in fractional calculus, which is a more generalized version of classical derivatives and integrals that involve real or complex number powers. This approach has proven to be effective in modeling a wide range of real-world problems across various fields, including physics, engineering, and science [4, 5, 6]. For instance, it has been used to model electromagnetic, thermodynamic, hydrodynamic, elastic, and fluid dynamic phenomena, as well as wave propagation, material science, and biological systems [7, 8, 9, 10, 11].

*Corresponding author: fozbag@harran.edu.tr

Fractional derivatives are a powerful mathematical tool that extend the concept of differentiation to non-integer orders [12, 13, 14, 15]. The different types of fractional derivatives, including the Riemann-Liouville, Grunwald-Letnikov, and Caputo derivatives, have different definitions and properties that make them suitable for different types of problems [16, 17]. The Caputo derivative is a popular choice in many applications due to its ability to accurately capture initial conditions and its mathematical properties that allow for easy incorporation into numerical methods. It allows for more physically meaningful initial conditions expressed in terms of integer-order derivatives. Unlike traditional derivatives, which are defined only for integer orders, Caputo fractional derivatives can be defined for any order between zero and one. This makes them useful in modeling systems that exhibit non-local and non-Markovian behavior, which cannot be described by traditional integer-order derivatives. One of the main benefits of using Caputo fractional derivatives is their ability to accurately model physical systems that exhibit memory effects. Memory effects refer to systems that retain information about their past state and history, which can significantly impact their future behavior. Traditional integer-order derivatives cannot account for these memory effects, but Caputo fractional derivatives can accurately capture the behavior of such systems.

The equation discussed in this article is an integro-differential equation that contains a fractional derivative in its integral term. Analytically solving these types of equations is often difficult, so accurate and efficient approximate solutions are necessary. This research introduces novel finite difference schemes, both first and second-order, aimed at addressing the initial-boundary value problem posed by fractional order integro-differential equations. Specifically, the study adopts the Caputo sense for fractional derivatives [18]. It carefully conducts error analyses for the numerical solutions, presenting results through both tabulated data and graphical representations. Moreover, the paper delves into von Neumann stability analyses concerning the finite difference scheme. To validate the accuracy of the proposed difference scheme, the research undertakes numerical experiments, comparing outcomes with exact solutions. The study compares the approximate solutions and exact solution for the same grid numbers for different fractional orders. Finally, the error graph shows that the solutions depend continuously on the fractional derivatives as the fractional order increases.

To ensure that the finite difference scheme used to approximate the solution of Caputo time fractional order hyperbolic integro-differential equations is stable, von Neumann stability analysis is commonly employed [19]. This analysis involves the use of Fourier analysis to derive a stability condition that must be satisfied by the finite difference scheme to ensure numerical stability. The von Neumann stability analysis is a powerful tool used to determine the stability of finite difference schemes for solving partial differential equations. It is an important aspect of numerical methods as it helps to ensure that the solutions obtained through finite difference methods are accurate and reliable.

The main contribution of the present work is the development and analysis of finite difference schemes for a class of fractional hyperbolic integro-partial differential equations. Unlike [20], which primarily focuses on the formulation and numerical treatment of related fractional problems, the present study constructs both first-order and second-order finite difference approximations for the considered model and investigates their numerical behavior. Furthermore, a stability restriction is derived through Fourier analysis, and

extensive numerical experiments are provided to compare the accuracy of the proposed schemes. The results demonstrate the effectiveness of the higher-order approximation in reducing the numerical error.

2. Problem statement and the necessary background information

We examine the subsequent problem, which involves a hyperbolic integro-differential equation of fractional order with an initial boundary condition.

$$\begin{cases} {}_0^C D_t^\beta z(t,x) + \int_0^t \gamma(\theta)\, {}_0^C D_\theta^\alpha z(\theta,x)\, d\theta = z_{xx}(t,x) + f(t,x), \\ z(0,x) = \phi(x), z_t(0,x) = 0, \quad 0 < x < L, \\ z(t,0) = z(t,L) = 0, \quad 0 < t < T, \\ 1 < \beta \leqslant 2, 0 < \alpha \leqslant 1 \end{cases} \tag{2.1}$$

In equation (2.1), $\phi(x)$ is given function and $\gamma(t)$ is defined as a continuous function on $(0,T]$. Following [20], we take

$$|\gamma(t)| \leqslant \frac{K}{t^{1-\alpha}}.$$

Also, ${}_0^C D_t^\alpha z(t,x)$ is known as the time fractional Caputo derivative of order α with the following definition [16]

$${}_0^C D_t^\alpha z(t,x) = \frac{1}{\Gamma(w-\alpha)} \int_0^t \frac{1}{(t-s)^{\alpha-w+1}} \frac{\partial^w z(s,x)}{\partial s^w} ds, \ (w-1 < \alpha \leqslant w) \tag{2.2}$$

where $\Gamma(\alpha) = \int_0^\infty s^{\alpha-1} e^{-s} ds$.

To solve problem (2.1) numerically, finite difference scheme method (FDS) will be utilized. To build finite difference scheme of (2.1), we give each terms finite difference equation. Firstly, let the uniform intervals for the x and t axes be defined as $h = \frac{L}{M}$ and $\tau = \frac{T}{N}$, respectively. In this case, $x_n = nh, n = 0,1,2,...,M$ and $t_k = k\tau, k = 0,1,2,...,N$ are obtained. For $1 < \beta \leqslant 2$ and $0 < \alpha \leqslant 1$, FDS of (2.2) is respectively

$${}_0^C D_t^\beta z(t,x) \approx \frac{\tau^{-\beta}}{\Gamma(3-\beta)} \sum_{j=0}^{k-1} ((j+1)^{2-\beta} - j^{2-\beta})(z_n^{k-j+1} - 2z_n^{k-j} + z_n^{k-j-1}), \tag{2.3}$$

$${}_0^C D_t^\alpha z(t,x) \approx \frac{\tau^{-\alpha}}{\Gamma(2-\alpha)} \sum_{j=0}^{k-1} ((j+1)^{1-\alpha} - j^{1-\alpha})(z_n^{k-j+1} - z_n^{k-j}). \tag{2.4}$$

First order FDS of z_{xx} is

$$z_{xx}(t_k, x_n) \approx \frac{z_{n+1}^k - 2z_n^k + z_{n-1}^k}{h^2} \tag{2.5}$$

In next section, by using (2.3), (2.4) and (2.5), we will construct first order FDS of (2.1) and analyze its stability by applying von-Neumann method.

3. Von-Neumann condition for the stability of finite difference scheme

Let $p_\beta = \frac{\tau^{-\beta}}{\Gamma(3-\beta)}$ and $b_{j,\beta} = (j+1)^{2-\beta} - j^{2-\beta}$, then using (2.3), (2.4) and (2.5) we discretize (2.1) into

$$\begin{cases} p_\beta \sum_{j=0}^{k-1} b_{j,\beta}(z_n^{k-j+1} - 2z_n^{k-j} + z_n^{k-j-1}) + \sum_{l=1}^{k-1}\sum_{m=1}^{l} \frac{\Gamma(l-m+1-\alpha)(z_n^m - z_n^{m-1})}{\Gamma(1-\alpha)(l-m)!l^{1-\alpha}} \\ = \frac{z_{n+1}^k - 2z_n^k + z_{n-1}^k}{h^2} + f_n^k, \\ x_n = nh, t_k = k\tau, 1 \leqslant k \leqslant N-1, \quad 1 \leqslant n \leqslant M-1, \\ z_n^0 = \phi(x_n), \quad \frac{z_n^1 - z_n^0}{\tau} = 0, \quad 0 \leqslant n \leqslant M, \\ z_0^k = z_M^k = 0, 0 \leqslant k \leqslant N. \end{cases} \tag{3.1}$$

The integral term involving the Caputo derivative is discretized using a quadrature rule based on the piecewise approximation of the fractional derivative kernel. Specifically, the time interval is partitioned uniformly with step size (τ), and the integral is approximated by applying a weighted summation over previous time levels. The resulting double summation structure naturally arises from substituting the discrete Caputo approximation into the integral operator. The detailed derivation of this discretization, including the role of the kernel function ($\gamma(t)$) and the associated scaling with respect to (τ), can be found in [20], where a similar construction is carried out for fractional integro-differential equations.

Remark. The von Neumann analysis presented below is performed for the principal discrete operator associated with the fractional hyperbolic part of the scheme. Following the approach adopted in [20], the memory term is treated as a nonlocal contribution whose coefficients remain bounded under the assumptions imposed on the kernel function ($\gamma(t)$). Consequently, the Fourier analysis is used to derive a practical stability restriction for the dominant finite-difference structure, while the influence of the memory term is assessed through numerical validation.

Theorem 3.1. *The difference scheme* (3.1) *is stable if the following condition holds*

$$h^2 \geqslant \tau^\beta \Gamma(3-\beta). \tag{3.2}$$

Proof. To analyze the stability of the scheme, we apply the Fourier (von Neumann) method. Let the numerical solution be expressed in the form

$$z_n^k = r^k e^{in\theta}, \qquad i = \sqrt{-1},$$

where r is the amplification factor and $\theta \in [0, \pi]$ is the wave number.

Substituting this form into the finite difference scheme and using the properties of the discrete Laplacian operator, we obtain the characteristic equation

$$r^2 - Ar + 1 = 0,$$

where

$$A = 2 - \frac{4\tau^\beta \Gamma(3-\beta)}{h^2} \sin^2\left(\frac{\theta}{2}\right).$$

The roots of the characteristic equation satisfy

$$r_1 + r_2 = A, \qquad r_1 r_2 = 1.$$

For stability, it is sufficient that the amplification factors remain bounded, i.e.

$$|r_1| \leqslant 1, \qquad |r_2| \leqslant 1.$$

This is guaranteed if

$$|A| \leqslant 2.$$

Indeed, when $|A| \leqslant 2$, the roots become complex conjugates:

$$r_{1,2} = \frac{A \pm i\sqrt{4 - A^2}}{2}.$$

Hence,

$$|r_{1,2}|^2 = \frac{A^2 + (4 - A^2)}{4} = 1,$$

which implies

$$|r_1| = |r_2| = 1.$$

Therefore, the Fourier modes remain bounded and the scheme is stable in the von Neumann sense.

Since

$$0 \leqslant \sin^2\left(\frac{\theta}{2}\right) \leqslant 1,$$

the most restrictive case occurs when

$$\sin^2\left(\frac{\theta}{2}\right) = 1.$$

Thus,

$$-2 \leqslant 2 - \frac{4\tau^\beta \Gamma(3-\beta)}{h^2} \leqslant 2.$$

From the left inequality, we obtain

$$\frac{4\tau^\beta \Gamma(3-\beta)}{h^2} \leqslant 4,$$

which yields the stability condition

$$h^2 \geqslant \tau^\beta \Gamma(3-\beta).$$

This completes the proof. □

The difference scheme (3.1) is stable if the condition (3.2) holds. Next section, we will test this with experimental validation confirming the accuracy of the proposed schemes against exact solutions.

4. Numerical results

This section provides comprehensive error analyses through tables and figures. An example is presented to confirm the stability condition and the accuracy of the first and second order FDS against exact solutions.

Hence, we proceed to investigate the following initial-boundary value problem, focusing on a fractional-order hyperbolic integro-differential equation, employing a numerical experiment as our investigative approach.

$$\begin{cases} {}_0^C D_t^\beta z(t,x) + \int_0^t \gamma(\theta)\, {}_0^C D_\theta^\alpha z(\theta,x)\, d\theta = z_{xx}(t,x) + f(t,x), \\ f(t,x) = (\frac{2t^{2-\beta}}{\Gamma(3-\beta)} + \frac{t^2}{\Gamma(3-\alpha)} + 2t^2 + 2)(x-x^2), 0 < x < 1, 0 < t < 1, \\ z(0,x) = x - x^2, z_t(0,x) = 0, \quad 0 \leqslant x \leqslant 1, \\ z(t,0) = z(t,1) = 0, \quad 0 \leqslant t \leqslant 1, \\ 1 < \beta \leqslant 2, 0 < \alpha \leqslant 1. \end{cases} \tag{4.1}$$

$z(t,x) = (t^2+1)(x-x^2)$ is the analytical solution of (4.1). It is easy to verify it by substituting into problem (4.1). By using (2.3), (2.4),(2.5) and the formula for second order FDS of z_{xx}

$$z_{xx}(t_k, x_n) \approx \frac{z_{n+1}^{k+1} - 2z_n^{k+1} + z_{n-1}^{k+1}}{2h^2} + \frac{z_{n+1}^{k-1} - 2z_n^{k-1} + z_{n-1}^{k-1}}{2h^2},$$

we give the following first and second order FDS of (4.1) to approximate the exact solution of it.

4.1. Truncation error and convergence analysis

To justify the accuracy of the proposed finite difference schemes, we analyze the local truncation error.

Let $z(t,x)$ be sufficiently smooth. Using Taylor expansion, we obtain for the spatial second derivative:

$$\frac{z(x+h) - 2z(x) + z(x-h)}{h^2} = z_{xx}(x) + \mathcal{O}(h^2). \tag{4.2}$$

Hence, the spatial discretization is second-order accurate in space.

For the Caputo time fractional derivative, using the L1-type approximation, it follows that

$${}_0^C D_t^\alpha z(t_k, x) = \frac{\tau^{-\alpha}}{\Gamma(2-\alpha)} \sum_{j=0}^{k-1} b_j \left(z^{k-j} - z^{k-j-1} \right) + \mathcal{O}(\tau^{2-\alpha}), \tag{4.3}$$

which implies first-order accuracy in time for $0 < \alpha \leqslant 1$.

Similarly, the approximation for $1 < \beta \leqslant 2$ satisfies

$${}_0^C D_t^\beta z(t_k, x) = \mathcal{O}(\tau^{3-\beta}), \tag{4.4}$$

which reduces to first-order accuracy in the considered range.

Therefore, the overall scheme achieves first-order accuracy in time and second-order accuracy in space.

4.2. First order accuracy

By using the following equations

$$ {}_0^C D_t^\beta z(t,x) \approx \frac{\tau^{-\beta}}{\Gamma(3-\beta)} \sum_{j=0}^{k-1} ((j+1)^{2-\beta} - j^{2-\beta})(z_n^{k-j+1} - 2z_n^{k-j} + z_n^{k-j-1}), \tag{4.5} $$

$$ {}_0^C D_t^\alpha z(t,x) \approx \frac{\tau^{-\alpha}}{\Gamma(2-\alpha)} \sum_{j=0}^{k-1} ((j+1)^{1-\alpha} - j^{1-\alpha})(z_n^{k-j+1} - z_n^{k-j}), \tag{4.6} $$

$$ z_{xx}(t_k, x_n) \approx \frac{z_{n+1}^k - 2z_n^k + z_{n-1}^k}{h^2} \tag{4.7} $$

and applying the similar procedure in [20], first order FDS of the problem is given by

$$ \begin{cases} p_\beta \sum_{j=0}^{k-l} b_{j,\beta}(z_n^{k-j+1} - 2z_n^{k-j} + z_n^{k-j-1}) + \sum_{l=1}^{k-1} \sum_{m=1}^{l} \frac{\Gamma(l-m+1-\alpha)(z_n^m - z_n^{m-1})}{\Gamma(1-\alpha)(l-m)!l^{1-\alpha}} \\ = \frac{z_{n+1}^k - 2z_n^k + z_{n-1}^k}{h^2} + f_n^k, \\ x_n = nh, t_k = k\tau, 1 \leqslant k \leqslant N-1, \quad 1 \leqslant n \leqslant M-1, \\ z_n^0 = x_n - x_n^2, \quad \frac{z_n^1 - z_n^0}{\tau} = 0, \quad 0 \leqslant n \leqslant M, \\ z_0^k = z_M^k = 0, 0 \leqslant k \leqslant N. \end{cases} \tag{4.8} $$

To solve the difference equation represented by equation (4.8) using the Gauss elimination method, we first express the system in matrix form. Equation (4.8) can be reformulated in matrix notation as follows:

Let Z_n and φ_n represent column vectors of size $(N+1) \times 1$ and A, B, C and D represent square matrices of size $(N+1) \times (N+1)$. The system can then be represented in matrix form as

$$ AZ_{n+1} + BZ_n + CZ_{n-1} = D\varphi_n. \tag{4.9} $$

The matrix formulation (4.9) is obtained by collecting the finite difference terms arising from the spatial discretization of the governing equation.

The contribution of the double summation term associated with the fractional integral operator is represented in matrix form following the construction given in [20, 21]. In particular, the convolution-type structure is transformed into a lower triangular Toeplitz-type matrix, as detailed therein.

The remaining matrices A, B, and C arise from the standard finite difference discretization of the time derivative and the spatial second-order derivative operator, which are well-known in classical finite difference formulations for parabolic and hyperbolic problems.

For clarity, the explicit construction of the double-sum matrix is omitted here to avoid repetition, while the standard components follow directly from the discretization procedure.

The error analysis of (4.9) is investigated by computing the maximum norm error between the approximate and exact solution with the following formula

$$\epsilon = \max_{\substack{1\leqslant k\leqslant N\\ 1\leqslant n\leqslant M}} |z(t,x) - z(t_k, x_n)|,$$

By fixing $\beta = 1.9$ and $\alpha = 0.9$, and for the values of N and M that satisfy the stability condition, we compute the maximum norm error of first order FDS (4.8) between the approximate and exact solution and present in Table 1. To support the Table 1 we also give some figures.

Table 1: Maximum Norm Errors for First Order FDS (4.8).

			$\tau = \frac{1}{N}$	$h = \frac{1}{M}$				
N	N=20	N=40	N=60	N=80	N=100	N=120	N=140	N=160
M	M=10	M=20	M=30	M=40	M=50	M=60	M=70	M=80
$\beta = 1.9$								
$\alpha = 0.9$	0.00505	0.00267	0.00184	0.00141	0.00114	0.00097	0.00084	0.00074

Table 1 presents the maximum norm errors for the first-order FDS for various combinations of N and M, which define the temporal and spatial grid resolutions. As N and M increase, corresponding to finer grids, the error decreases steadily. This demonstrates the convergence of the method, as the numerical solution becomes more accurate with finer discretization. The errors remain small throughout, confirming the validity of the first-order scheme. The error graph corresponding to the error Table 1 is presented in Figure 1. The errors exhibit a decreasing trend as the time values change. The decreasing trend supports the reliability of the method for longer time simulations.

To further verify the convergence behavior of the proposed scheme, additional numerical experiments were performed by varying the spatial and temporal discretization parameters independently. The experimental order of convergence (EOC) is computed by

$$\text{EOC} = \frac{\log(E_1/E_2)}{\log(h_1/h_2)}, \tag{4.10}$$

where E_1 and E_2 denote the numerical errors corresponding to two successive mesh refinements. For the temporal convergence study, the same formula is used with the time step size τ replacing h.

First, the temporal discretization parameter is fixed at $M = 20$, while the spatial mesh is successively refined. The corresponding errors and experimental orders of convergence are reported in Table 2.

Table 2: Spatial convergence study for the first-order scheme with $M = 20$.

N	Error	Order
30	0.0034737	–
40	0.0026696	0.9152
50	0.0021758	0.9166
60	0.0018414	0.9153
70	0.0015986	0.9173
80	0.0014139	0.9195
90	0.0012685	0.9213
100	0.0011511	0.9218

The obtained orders are close to unity, indicating that the proposed finite difference scheme achieves first-order spatial accuracy.

Next, the spatial discretization parameter is fixed at $N = 100$, while the temporal mesh is refined. The corresponding results are presented in Table 3.

Table 3: Temporal convergence study for the first-order scheme with $N = 100$.

M	Error	Order
20	0.002735	–
30	0.0021023	0.912
40	0.0015637	0.913
50	0.0011497	0.915
60	0.0008096	0.917
70	0.0006496	0.919
80	0.0005052	0.920

The experimental temporal convergence orders are also approximately equal to one. Therefore, the proposed numerical scheme exhibits first-order convergence in both space and time, which is consistent with the theoretical accuracy of the method.

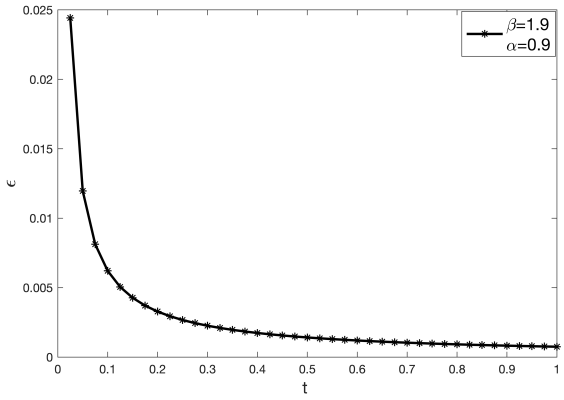

Figure 1: Maximum norm errors as t changes for (4.8).

Figure 2 compares the approximate solution obtained from the first-order scheme with the exact analytical solution at a fixed time and space grid. In Figure 2 the two curves are almost indistinguishable, highlighting the high accuracy of the numerical method. This figure provides visual confirmation of the small errors reported in Table 1.

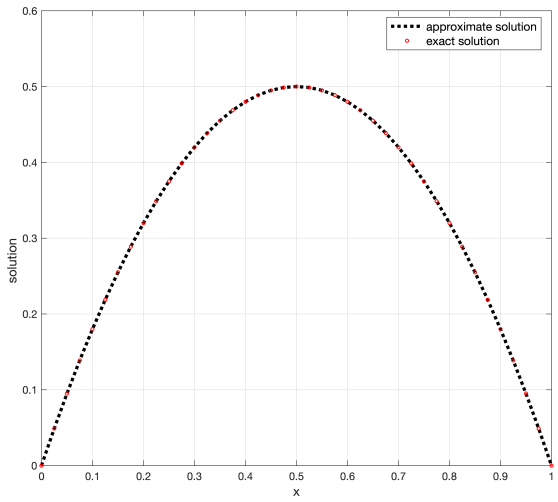

Figure 2: $\beta = 1.9$, $\alpha = 0.9$, $N = 80$ and $M = 40$ for (4.8) .

Figure 3 illustrates how the maximum error changes when the fractional order α varies, while keeping β and grid parameters fixed. The smooth dependence of error on α demonstrates the continuous sensitivity of the numerical solution to fractional order parameters, as expected in fractional models capturing memory effects.

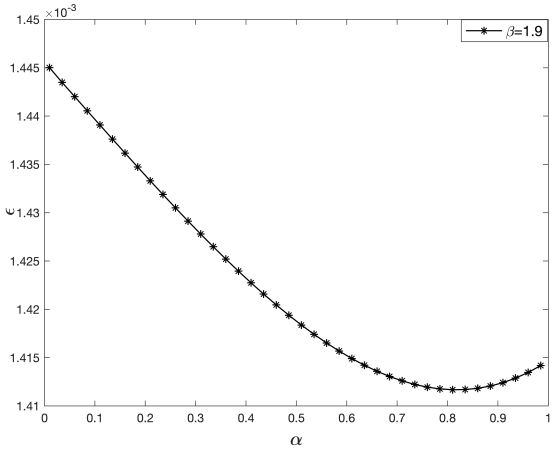

Figure 3: Set $\beta = 1.9$, $N = 80$ and $M = 40$.

4.3. Second order accuracy

Similarly, second order FDS of the problem is given by

$$\begin{cases} p_\beta \sum_{j=0}^{k-l} b_{j,\beta}(z_n^{k-j+1} - 2z_n^{k-j} + z_n^{k-j-1}) + \sum_{l=1}^{k-1}\sum_{m=1}^{l} \frac{\Gamma(l-m+1-\alpha)(z_n^m - z_n^{m-1})}{\Gamma(1-\alpha)(l-m)!l^{1-\alpha}} \\ = \frac{z_{n+1}^{k+1} - 2z_n^{k+1} + z_{n-1}^{k+1}}{2h^2} + \frac{z_{n+1}^{k-1} - 2z_n^{k-1} + z_{n-1}^{k-1}}{2h^2} + f_n^k, \\ x_n = nh, t_k = k\tau, 1 \leqslant k \leqslant N-1, \quad 1 \leqslant n \leqslant M-1, \\ z_n^0 = x_n - x_n^2, \quad \frac{z_n^2 - 4z_n^1 + 3z_n^0}{2\tau} = 0, \quad 0 \leqslant n \leqslant M, \\ z_0^k = z_M^k = 0, 0 \leqslant k \leqslant N. \end{cases} \tag{4.11}$$

The proposed second-order scheme achieves second-order accuracy in space, while the time discretization of the fractional derivative is based on a high-order approximation. However, due to the presence of the Caputo fractional derivative, the overall temporal accuracy is generally limited by the regularity of the solution and the memory effect. Therefore, the scheme should be interpreted as a higher-order spatial discretization combined with a fractional time approximation.

By fixing $\beta = 1.9$ and $\alpha = 0.9$, and for the values of N and M , we calculate the numerical error of second order FDS (4.11) between the approximate and exact solution and present in Table 4. Compared to Table 1, errors are significantly smaller for the same grid parameters, verifying that the second-order scheme offers superior accuracy. The data further affirm that error decreases with mesh refinement, consistent with the theoretical expectations for a second-order method.

Table 4: Maximum Norm Errors for Second Order FDS (4.11).

			$\tau = \frac{1}{N}$	$h = \frac{1}{M}$				
N	N=20	N=40	N=60	N=80	N=100	N=120	N=140	N=160
M	M=10	M=20	M=30	M=40	M=50	M=60	M=70	M=80
$\beta = 1.9$								
$\alpha = 0.9$	0.00266	0.00123	0.00083	0.00063	0.00052	0.00044	0.00038	0.00034

We also plot error graph of (4.11) in Figure 4. Figure 4 shows the maximum norm error over time for the second-order scheme. The error is notably lower than that of the first-order method and consistently decreases as time increases, emphasizing the enhanced precision and stability of the second-order scheme throughout the computational domain.

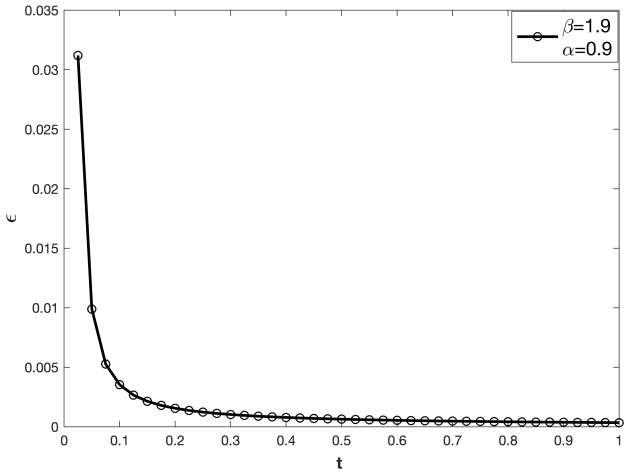

Figure 4: Maximum norm errors as t changes for (4.11).

In Figure 5, numerically computed solution almost fits with the exact solution. The precision level of the second order FDS is again much higher than that of the first order FDS.

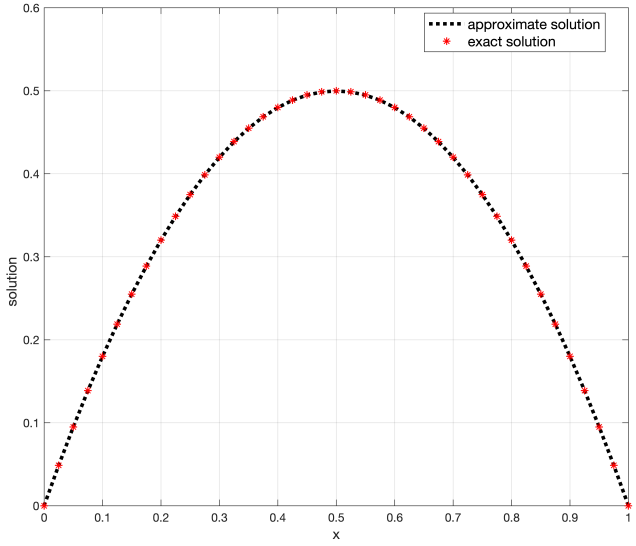

Figure 5: $\beta = 1.9$, $\alpha = 0.9$, N $= 80$ and M $= 40$ for (4.11).

5. Conclusion

This paper presented first- and second-order finite difference schemes for a class of fractional hyperbolic integro-partial differential equations involving a Caputo fractional derivative. Stability restrictions were derived through Fourier analysis and supported by numerical experiments. The computed results demonstrated convergence of the proposed methods and showed that the second-order scheme provides significantly improved accuracy compared with the first-order approximation. The numerical solutions were found to be in excellent agreement with the exact solution, confirming the effectiveness of the proposed approach for solving fractional integro-differential models.

Conflict of interest: The author has no conflict of interest to declare.
Funding: No funding was received.

References

[1] Ozbag F (2022). *Numerical simulations of traveling waves in a counterflow filtration combustion model*. Turk. J. Math., **46**: 1424–1435.
[2] Lin Z and Wang H (2021). *Modeling and application of fractional-order economic growth model with time delay*. Fractal Fract., **5**: 74. https://doi.org/10.3390/fractalfract5030074
[3] Taubes C (2008). *Modeling Differential Equations in Biology*. Cambridge: Cambridge University Press.
[4] Hilfer R (2000). *Applications of Fractional Calculus in Physics*. River Edge, NJ, USA: World Scientific Publishing.
[5] Jannelli A (2020). *Numerical solutions of fractional differential equations arising in engineering sciences*. Mathematics, **8**: 215. https://doi.org/10.3390/math8020215
[6] Sokolov IM, Klafter J and Blumen A (2002). *Fractional kinetics*. Phys. Today, **55**: 48–54. https://doi.org/10.1063/1.1535007
[7] Tarasov VE (2009). *Fractional integro-differential equations for electromagnetic waves in dielectric media*. Theor. Math. Phys., **158**: 355–359. https://doi.org/10.1007/s11232-009-0030-7
[8] Momani S and Odibat Z (2006). *Analytical approach to linear fractional partial differential equations arising in fluid mechanics*. Phys. Lett. A, **355**: 271–279. https://doi.org/10.1016/j.physleta.2006.02.048
[9] Ozbag F and Schecter S (2018). *Stability of combustion waves in a simplified gas-solid combustion model in porous media*. Philos. Trans. R. Soc. A, **376**(2117): 20170185. https://doi.org/10.1098/rsta.2017.0185
[10] He JH and Ji FY (2019). *Two-scale mathematics and fractional calculus for thermodynamics*. Therm. Sci., **23**: 2131–2133. https://doi.org/10.2298/TSCI1904131H
[11] Cattani C, Srivastava HM and Yang XJ (2016). *Fractional Dynamics*. Berlin: de Gruyter.
[12] Yang X (2019). *General Fractional Derivatives: Theory, Methods and Applications*. New York: CRC Press.
[13] Lachouri A, Abdo MS and Ardjouni A (2024). *On a class of system of generalized neutral hyperbolic partial fractional differential equations*. Nonlinear Studies, **31**(1).
[14] Wahash HA, Abdo MS, Saeed AM and Panchal SK (2020). *Singular fractional differential equations with ψ-Caputo operator and modified Picard's iterative method*. Appl. Math. E-Notes, **20**: 215–229.
[15] Abdo MS and Panchal SK (2018). *Some new uniqueness results of solutions to nonlinear fractional integro-differential equations*. Annals of Pure and Applied Mathematics, **16**(2): 345–352.
[16] Podlubny I (1998). *Fractional Differential Equations: An Introduction to Fractional Derivatives, Fractional Differential Equations, to Methods of Their Solution and Some of Their Applications*. San Diego: Academic Press, Vol. 198.
[17] Samko SG, Kilbas AA and Marichev OI (1993). *Fractional Integrals and Derivatives: Theory and Applications*. Langhorne: Gordon and Breach.
[18] Caputo M (1967). *Linear models of dissipation whose Q is almost frequency independent*. Geophys. J. Int., **13**: 529–539. https://doi.org/10.1111/j.1365-246X.1967.tb02303.x

[19] Yuste SB and Acedo L (2005). *An explicit finite difference method and a new von Neumann-type stability analysis for fractional diffusion equations*. SIAM J. Numer. Anal., **42**: 1862–1874. https://doi.org/10.1137/S0036142903422301

[20] Hicdurmaz B (2015). *Initial boundary value problems for fractional Schrödinger differential equations*. PhD Thesis, Gebze Technical University.

[21] Ozbag F (2026). *Stability and Numerical Simulation of 2D Fractional Pseudo-Hyperbolic Partial Differential Equations*. Journal of Mathematics and Statistics Studies, **7**(4): 18–24.